Eur. Phys. J. B **22**, 167–178 (2001)

THE EUROPEAN PHYSICAL JOURNAL B

EDP Sciences

Thermodynamics and optical conductivity of unconventional spin density waves

B. Dóra[1] and A. Virosztek[1,2,a]

[1] Department of Physics, Technical University of Budapest, 1521 Budapest, Hungary
[2] Research Institute for Solid State Physics and Optics, PO Box 49, 1525 Budapest, Hungary

Received 19 February 2001

Abstract. We consider the possibility of formation of an unconventional spin density wave (USDW) in quasi-one-dimensional electronic systems. In analogy with unconventional superconductivity, we develop a mean field theory of SDW allowing for the momentum dependent gap $\Delta(\mathbf{k})$ on the Fermi surface. Conditions for the appearance of such a low temperature phase are investigated. The excitation spectrum and basic thermodynamic properties of the model are found to be very similar to those of d-wave superconductors in spite of the different topology of their Fermi surfaces. Several correlation functions are calculated, and the frequency dependent conductivity is evaluated for various gap functions. The latter is found to reflect the maximum gap value, however with no sharp onset for absorbtion.

PACS. 75.30.Fv Spin-density waves – 71.45.Lr Charge-density-wave systems – 78.30.Jw Organic compounds, polymers

1 Introduction

As a result of intense research during the past few decades, much is known about the properties of density waves possessing a constant Δ order parameter [1]. On the other hand it is well known that wavevector dependent order parameters $\Delta(\mathbf{k})$ taking different values at different points on the Fermi surface play an important role in theories of superconductivity (termed unconventional) [2] in various systems including the high-T_c cuprates [3]. Therefore the need to work out the theory of unconventional density waves follows naturally from these precedents.

This project however is not just of academic interest. Heavy-fermion compounds have long been suspected of possibly having wavevector dependent SDW gap on a three-dimensional nested Fermi surface [4]. The anomalously small magnetic moment in URu_2Si_2 [5] was suggested to be explained among other possibilities [6,7] by unconventional SDW on a quasi-two-dimensional (square) Fermi surface [8]. The basis of this suggestion is the fact that an USDW is in fact not a spin density wave at all, since it is not accompanied by periodic spin density modulation. The order parameter of the phase transition is not the spin density itself, but another well defined quantity related to the spin density much the same way as the "effective density" responsible for electronic Raman scattering is related to the density operator [9,10]. As another signature of an unconventional density wave (DW), low energy excitations due to a DW gap vanishing on certain subsets of the Fermi surface may be responsible for the absence of a clear optical gap in the reflectivity data of some of the heavy-electron materials [11], including URu_2Si_2. Optical data with similar features in the low temperature phase of quasi-one-dimensional Mo_4O_{11} indicate again the possibility of an unconventional charge density wave (UCDW) state [12,13].

Other candidates for unconventional DW states include the organic conductor α-(BEDT-TTF)$_2$KHg(SCN)$_4$, where in spite of a clear indication for a phase transition in magnetotransport measurements neither charge nor magnetic order has been established [14–16], the transition-metal dichalcogenide 2H-$TaSe_2$ with its momentum dependent CDW gap inferred from angle resolved photoemission studies [17], and the tetrachalcogenide $(TaSe_4)_2I$, for which the magnetic susceptibility above the conventional CDW transition temperature shows pseudogap behavior [18,19] without any observable long range charge order. Indeed, a recent suggestion to understand the pseudogap phase of the cuprate superconductors also invokes the existence of an unconventional density wave (UDW) of d-symmetry [20]. Motivated partly by the rich phase diagram of the high T_c cuprates, significant steps have already been made towards the theory of UDW in a two-dimensional electron system [21], typically on a square lattice [22].

Momentum dependent order parameter in an electron-hole condensate was first introduced in the context of the excitonic insulator [23]. Further studies [24,25] were initiated by the discovery of high-T_c superconductors, and the

[a] e-mail: viro@szfki.hu

orbital antiferromagnetic phase on a square lattice was proposed [26]. The magnetic response of the orbital antiferromagnet [27] and the so called spin nematic phase [28] was investigated in a two-dimensional system, as well as in a two chain ladder [29].

The objective of the present paper is to make the first steps in developing a detailed theory of UDW-s in quasi-one-dimensional interacting electron systems. Clearly, the topology of the Fermi surface is radically different in this problem than in previous treatments, moreover the strong anisotropy of transport properties in, and perpendicular to the linear chain direction is of particular interest. A preliminary report of some of our results has already been published [30]. The article is organized as follows: in Section 2 we define our model, develop its thermodynamics in mean field theory, and determine conditions for the appearance of USDW. Section 3 is devoted to the calculation of the most important correlation functions of the system, while in Section 4 we pay particular attention to the optical conductivity of the model. Our conclusions are given in Section 5.

2 Thermodynamics of the model

We start with a quasi-one-dimensional interacting electron system described by the following one band Hamiltonian:

$$H = \sum_{\mathbf{k},\sigma} \varepsilon(\mathbf{k}) a^+_{\mathbf{k},\sigma} a_{\mathbf{k},\sigma} + \frac{1}{2V} \sum_{\substack{\mathbf{k},\mathbf{k}',\mathbf{q} \\ \sigma,\sigma'}} \tilde{V}(\mathbf{k},\mathbf{k}',\mathbf{q}) a^+_{\mathbf{k}+\mathbf{q},\sigma} a_{\mathbf{k},\sigma} a^+_{\mathbf{k}'-\mathbf{q},\sigma'} a_{\mathbf{k}',\sigma'}, \quad (1)$$

where $a^+_{\mathbf{k},\sigma}$ and $a_{\mathbf{k},\sigma}$ are creation and annihilation operators of an electron of momentum $\mathbf{k}$ and spin σ, V is the volume of the sample and the kinetic energy spectrum on an orthorhombic lattice

$$\epsilon(\mathbf{k}) = -2t_a \cos(k_x a) - 2t_b \cos(k_y b) - 2t_c \cos(k_z c) - \mu \quad (2)$$

is highly anisotropic ($t_a \gg t_b, t_c$). The interaction potential matrix elements in (1) are:

$$\frac{1}{V}\tilde{V}(\mathbf{k},\mathbf{k}',\mathbf{q}) = \int \mathrm{d}^3 r \int \mathrm{d}^3 r' \bar{\varphi}_{\mathbf{k}+\mathbf{q}}(\mathbf{r}) \bar{\varphi}_{\mathbf{k}'-\mathbf{q}}(\mathbf{r}') V(\mathbf{r}-\mathbf{r}') \varphi_{\mathbf{k}'}(\mathbf{r}') \varphi_{\mathbf{k}}(\mathbf{r}), \quad (3)$$

where $\varphi_{\mathbf{k}}$ is Bloch function. In Wannier basis $\varphi_{\mathbf{k}}(\mathbf{r}) = \frac{1}{\sqrt{N}} \sum_{\mathbf{R}} \mathrm{e}^{\mathrm{i}\mathbf{k}\mathbf{R}} \varphi(\mathbf{r}-\mathbf{R})$, where N is the number of cells and $\varphi(\mathbf{r})$ is the corresponding Wannier function assumed to be real and an eigenfunction of parity. We note here that in a tight-binding solid the Wannier function is well localized, leading to a significant dependence of the interaction matrix element (3) on the incoming electron momenta $\mathbf{k}$ and $\mathbf{k}'$. This turns out to be crucial in order to form an UDW, and is readily seen from the expansion including on site and nearest neighbor two center integrals:

$$\begin{aligned}\frac{N}{V}\tilde{V}(\mathbf{k},\mathbf{k}',\mathbf{q},\sigma,\sigma') = \delta_{-\sigma,\sigma'} \Big\{ U + \sum_i [& 2V_i \cos q_i \delta_i \\ & + 2J_i \cos(k_i - k'_i + q_i)\delta_i \\ & + 2F_i \cos(k'_i + k_i)\delta_i \\ & + 2C_i(\cos k_i \delta_i + \cos k'_i \delta_i \\ & + \cos(k'_i - q_i)\delta_i + \cos(k_i + q_i)\delta_i)] \Big\} \\ & + \delta_{\sigma,\sigma'} \sum_i (V_i - J_i)(\cos q_i \delta_i \\ & - \cos(k_i - k'_i + q_i)\delta_i). \end{aligned} \quad (4)$$

In the above formula the antisymmetrized (therefore spin dependent) interaction is given with $i = x, y, z$ and $\delta_i = a, b, c$. The (at most) two center integrals are the on site Hubbard repulsion and the nearest neighbor direct, exchange, pair-hopping and bond-charge terms

$$U = \int \mathrm{d}^3 r \int \mathrm{d}^3 r' |\varphi(\mathbf{r})|^2 V(\mathbf{r}-\mathbf{r}') |\varphi(\mathbf{r}')|^2, \quad (5a)$$

$$V_i = \int \mathrm{d}^3 r \int \mathrm{d}^3 r' |\varphi(\mathbf{r})|^2 V(\mathbf{r}-\mathbf{r}') |\varphi(\mathbf{r}'-\mathbf{e}_i)|^2, \quad (5b)$$

$$J_i = \int \mathrm{d}^3 r \int \mathrm{d}^3 r' \bar{\varphi}(\mathbf{r}) \bar{\varphi}(\mathbf{r}'-\mathbf{e}_i) V(\mathbf{r}-\mathbf{r}') \varphi(\mathbf{r}') \varphi(\mathbf{r}-\mathbf{e}_i), \quad (5c)$$

$$F_i = \int \mathrm{d}^3 r \int \mathrm{d}^3 r' \bar{\varphi}(\mathbf{r}) \bar{\varphi}(\mathbf{r}')\, V(\mathbf{r}-\mathbf{r}') \varphi(\mathbf{r}'-\mathbf{e}_i) \varphi(\mathbf{r}-\mathbf{e}_i), \quad (5d)$$

$$C_i = \int \mathrm{d}^3 r \int \mathrm{d}^3 r' \bar{\varphi}(\mathbf{r}) \bar{\varphi}(\mathbf{r}')\, V(\mathbf{r}-\mathbf{r}') \varphi(\mathbf{r}') \varphi(\mathbf{r}-\mathbf{e}_i), \quad (5e)$$

where $\mathbf{e}_i$ is the lattice vector in the i-direction.

Although due to its rich structure the interaction in equation (4) is able to support a variety of low temperature phases [31] depending on the Hubbard integrals in equation (5), we are now interested in constructing the mean field theory of an USDW. The best nesting vector for the spectrum (2) is obviously $\mathbf{Q} = (2k_\mathrm{F}, \pi/b, \pi/c)$ with the Fermi wavenumber k_F satisfying $\mu = -2t_a \cos(ak_\mathrm{F})$. In a DW expectation values of the type $\langle a^+_{\mathbf{k},\sigma} a_{\mathbf{k}+\mathbf{Q},\sigma} \rangle$ will not vanish, defining the order parameter of the low temperature phase $\Delta(\mathbf{k},\sigma) = |\Delta(\mathbf{k},\sigma)| \mathrm{e}^{\mathrm{i}\phi(\mathbf{k},\sigma)}$ as

$$\Delta(\mathbf{k},\sigma) = \frac{1}{V} \sum_{\mathbf{k}',\sigma'}'' \overline{\tilde{V}(\mathbf{k}',\mathbf{k},\mathbf{Q},\sigma,\sigma')} \langle a^+_{\mathbf{k}',\sigma'} a_{\mathbf{k}'+\mathbf{Q},\sigma'} \rangle. \quad (6)$$

Here the overline indicates complex conjugation and the double prime over the summation sign restricts k_x values to the interval from $-2k_\mathrm{F}$ to 0. Then the mean field Hamiltonian is diagonalized in the usual way, giving rise to a two band quasiparticle spectrum over the new Brillouin

zone ($0 < k_x < 2k_\mathrm{F}$) given by

$$E_\pm(\mathbf{k}) = \frac{\varepsilon(\mathbf{k}) + \varepsilon(\mathbf{k}-\mathbf{Q})}{2} \pm \sqrt{\left(\frac{\varepsilon(\mathbf{k}) - \varepsilon(\mathbf{k}-\mathbf{Q})}{2}\right)^2 + |\Delta(\mathbf{k},\sigma)|^2}. \quad (7)$$

The new (effectively noninteracting) fermionic quasiparticles are expressed by the original electrons as

$$\begin{aligned} d_{+\mathbf{k}\sigma} &= \mathrm{e}^{-\mathrm{i}\phi(\mathbf{k},\sigma)} u(\mathbf{k},\sigma) a_{\mathbf{k},\sigma} + v(\mathbf{k},\sigma) a_{\mathbf{k}-\mathbf{Q},\sigma}, \\ d_{-\mathbf{k}\sigma} &= \mathrm{e}^{-\mathrm{i}\phi(\mathbf{k},\sigma)} v(\mathbf{k},\sigma) a_{\mathbf{k},\sigma} - u(\mathbf{k},\sigma) a_{\mathbf{k}-\mathbf{Q},\sigma}, \end{aligned} \quad (8)$$

with

$$\begin{matrix} u(\mathbf{k},\sigma) \\ v(\mathbf{k},\sigma) \end{matrix} = \sqrt{\frac{1}{2}\left(1 \pm \frac{\frac{\varepsilon(\mathbf{k})-\varepsilon(\mathbf{k}-\mathbf{Q})}{2}}{\sqrt{(\frac{\varepsilon(\mathbf{k})-\varepsilon(\mathbf{k}-\mathbf{Q})}{2})^2 + |\Delta(\mathbf{k},\sigma)|^2}}\right)}. \quad (9)$$

Equations (6) and (8) lead to a self consistency condition for the order parameter known as the gap equation

$$\Delta(\mathbf{l},\sigma') = {\sum_{\mathbf{k},\sigma}}' \frac{1}{V} \overline{\tilde{V}(\mathbf{k}-\mathbf{Q},\mathbf{l},\mathbf{Q},\sigma',\sigma)} \times \frac{\Delta(\mathbf{k},\sigma)\{f[E_+(\mathbf{k},\sigma)] - f[E_-(\mathbf{k},\sigma)]\}}{2\sqrt{(\frac{\varepsilon(\mathbf{k})-\varepsilon(\mathbf{k}-\mathbf{Q})}{2})^2 + |\Delta(\mathbf{k},\sigma)|^2}}, \quad (10)$$

where the prime indicates that the $\mathbf{k}$ sum runs over the new Brillouin zone only, and $f(E)$ is the Fermi function.

In the followings we suppress the spin index of the order parameter, since in order to describe an SDW with polarization vector parallel to the z-axis of the spin space, we can utilize the relation $\Delta(\mathbf{k},+) = -\Delta(\mathbf{k},-) = \Delta(\mathbf{k})$. Moreover, the structure of the gap equation makes it clear that the relevant wavenumber values in the arguments of both the gap and the interaction are confined to a narrow region near the Fermi sheet at $+k_\mathrm{F}$. Therefore the gap equation is in fact an integral equation on the $k_x = k_\mathrm{F}$ plane of variables k_y and k_z only. Making use of the electron spectrum (2) linearized in k_x around k_F: $\xi(\mathbf{k}) = v_\mathrm{F}(k_x - k_\mathrm{F}) - 2t_b\cos(k_y b) - 2t_c\cos(k_z c)$, we obtain a simplified gap equation ($v_\mathrm{F} = 2at_a\sin(ak_\mathrm{F})$ is the Fermi velocity):

$$\begin{aligned} \Delta(\mathbf{l}) &= {\sum_{\mathbf{k}}}' \frac{1}{V} \overline{P(\mathbf{k},\mathbf{l})} \frac{\Delta(\mathbf{k}) \tanh\left\{\frac{\beta}{2}E(\mathbf{k})\right\}}{2E(\mathbf{k})} \\ &\approx \int_{-\pi/b}^{\pi/b} \frac{\mathrm{d}k_y}{2\pi} \int_{-\pi/c}^{\pi/c} \frac{\mathrm{d}k_z}{2\pi} \int_0^{v_\mathrm{F}k_\mathrm{F}} \frac{\mathrm{d}\xi}{2\pi v_\mathrm{F}} \overline{P(\mathbf{k},\mathbf{l})} \Delta(\mathbf{k}) \\ &\quad \times \frac{\tanh\left\{\frac{\beta}{2}\sqrt{\xi^2 + |\Delta(\mathbf{k})|^2}\right\}}{\sqrt{\xi^2 + |\Delta(\mathbf{k})|^2}}. \end{aligned} \quad (11)$$

Here $E(\mathbf{k}) = \sqrt{[\xi(\mathbf{k})]^2 + |\Delta(\mathbf{k})|^2}$, $\beta = 1/k_\mathrm{B}T$, we have neglected terms of order $(t_{b,c}/t_a)^2$ in the second expression, and the kernel of the integral equation is

$$\begin{aligned} \frac{P(\mathbf{k},\mathbf{l})}{V} &= \frac{P_0}{N} + \frac{P_1}{N}\cos(k_y b)\cos(l_y b) \\ &\quad + \frac{P_2}{N}\sin(k_y b)\sin(l_y b) + \frac{P_3}{N}\cos(k_z c)\cos(l_z c) \\ &\quad + \frac{P_4}{N}\sin(k_z c)\sin(l_z c), \end{aligned} \quad (12)$$

with coefficients given by

$$\begin{aligned} P_0 &= U - V_y - V_z - J_y - J_z \\ &\quad + (V_x + J_x)(\cos(2k_\mathrm{F}a) + 1) + 2F_x + 8C_x\cos(k_\mathrm{F}a), \end{aligned} \quad (13a)$$

$$P_1 = -2F_y + J_y + V_y, \quad (13b)$$

$$P_2 = 2F_y + J_y + V_y, \quad (13c)$$

$$P_3 = -2F_z + J_z + V_z, \quad (13d)$$

$$P_4 = 2F_z + J_z + V_z. \quad (13e)$$

As is seen above in equation (12), the kernel turns out to be diagonal on the basis of the leading harmonics on the (k_y, k_z) plane. Consequently, the gap will be of the form

$$\Delta(\mathbf{k}) = \Delta_0 + \Delta_1\cos(k_y b) + \Delta_2\sin(k_y b) + \Delta_3\cos(k_z c) + \Delta_4\sin(k_z c). \quad (14)$$

For vanishing order parameter the five components in (11) decouple completely, and the critical temperature for the development of each type of gap can easily be evaluated. For the conventional SDW with constant gap we recover the well known result

$$k_\mathrm{B}T_\mathrm{c}^{(0)} = \frac{2\gamma}{\pi} v_\mathrm{F} k_\mathrm{F} \mathrm{e}^{-2/P_0\rho_0(0)}, \quad (15)$$

with $\gamma = 1.781$, the Euler constant, and $\rho_0(0) = a/\pi v_\mathrm{F}$ is the electron density of states in the normal state per spin at the Fermi surface. The critical temperature for the four kinds of unconventional gap formation ($j = 1, ..., 4$) is

$$k_\mathrm{B}T_\mathrm{c}^{(j)} = \frac{2\gamma}{\pi} v_\mathrm{F} k_\mathrm{F} \mathrm{e}^{-4/P_j\rho_0(0)}. \quad (16)$$

On cooling the system, that type of an SDW will develop first, for which the T_c is the highest. The condition for the formation of an USDW of type j is $P_j > 2P_0$. For example in case of a half filled band an unconventional phase with the gap function $\Delta(\mathbf{k}) = \Delta_2\sin(bk_y)$ will form if $\frac{3}{2}(V_y + J_y) + F_y + V_z + J_z > U + 2F_x$. Clearly, a combination of interchain Coulomb and exchange integrals overwhelming the on site repulsion will facilitate the development of an USDW (negative interchain pair-hopping integral favours a gap with cosine dependence) instead of a conventional SDW. It may be of interest to consider the competition with CDW instabilities as well. The effective couplings for a conventional CDW and for a UCDW are $P_\mathrm{CDW} = -(U + 2F_x - 4V_x + 4J_x - 3V_y - 3V_z + J_y + J_z)$ and $P_\mathrm{UCDW} = V_y - 3J_y \pm 2F_y$ respectively, where the upper and lower sign refers to a k_y dependent gap function of cosine and sine

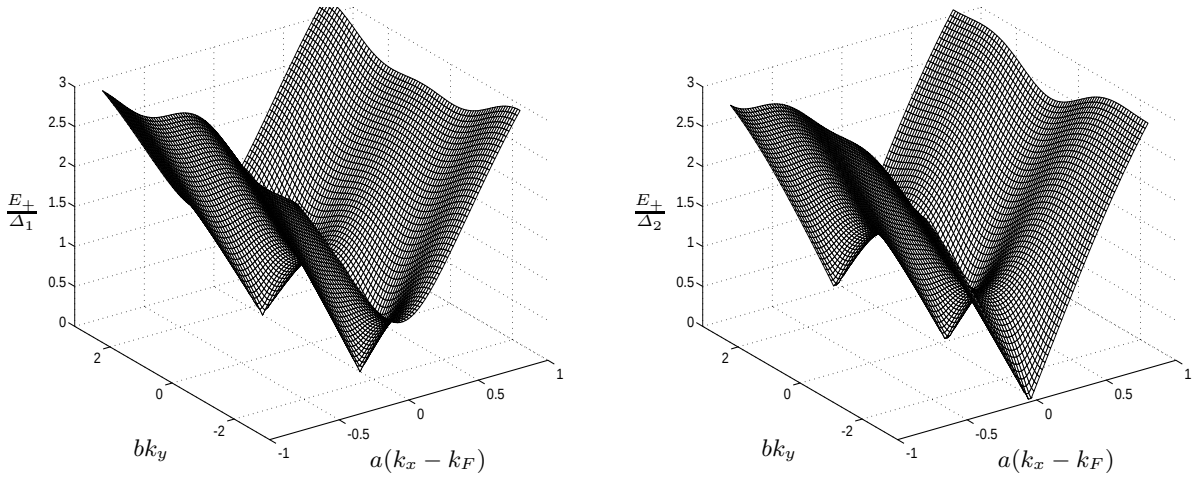

Fig. 1. Quasiparticle energy spectrum of an USDW. $E_+(\mathbf{k})$ is given for $\Delta(\mathbf{k}) = \Delta_1 \cos(bk_y)$ (left panel), and for $\Delta(\mathbf{k}) = \Delta_2 \sin(bk_y)$ (right panel). Other parameters are chosen as $t_a/\Delta_{1,2} = 2$, $t_b/\Delta_{1,2} = 0.1$ and $ak_{\rm F} = \pi/2$.

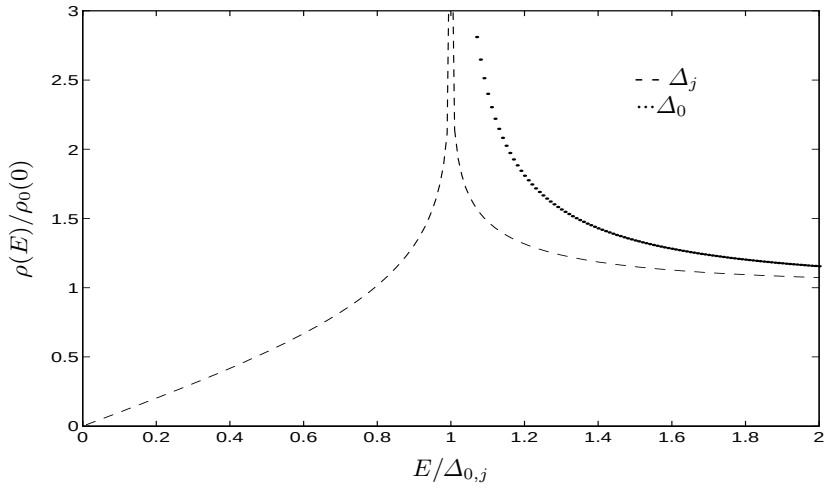

Fig. 2. The density of states for conventional (dotted line), and unconventional (dashed line) density waves.

form. In particular, we obtain that the USDW is stable with respect to the UCDW if $J_y \mp F_y > 0$.

The quasiparticle energy spectrum from equation (7) is shown in Figure 1 for the two typical unconventional gap functions of k_y (we neglected any dispersion in k_z here for clarity). The excitation energy vanishes on lines (note the additional k_z-direction in the Brillouin zone) of the Fermi surface, and this will determine the nature of the thermodynamics of the system. The corresponding density of states (DOS) is calculated as

$$\frac{\rho(E)}{\rho_0(0)} = \int_{-\pi}^{\pi} \frac{\mathrm{d}(bk_y)}{2\pi} \int_{-\pi}^{\pi} \frac{\mathrm{d}(ck_z)}{2\pi} \mathrm{Re} \frac{|E|}{\sqrt{E^2 - |\Delta(\mathbf{k})|^2}}, \tag{17}$$

and is shown in Figure 2 for both the well known conventional situation and for the unconventional cases determined analytically by $\rho(E)/\rho_0(0) = (2|E|/\pi|\Delta_j|) \times K(|E|/|\Delta_j|)$ if $|E| < |\Delta_j|$, and $\rho(E)/\rho_0(0) = (2/\pi)K(|\Delta_j|/|E|)$ if $|E| > |\Delta_j|$. In the latter case the DOS vanishes linearly at the Fermi energy and diverges logarithmically at the maximum gap value, as follows from the properties of the complete elliptic function of the first kind.

Assuming that only one kind of gap (either the conventional or one of the four unconventionals, whichever opens at the highest $T_{\rm c}$) persists all the way down to zero temperature, we can use equation (11) in order to evaluate the temperature dependence of the gap amplitude. This is the same for all unconventional gap types, and is shown on Figure 3 along with the conventional dependence, displaying only small differences between the two. At zero temperature the unconventional gap takes the value $|\Delta_j(0)| = (2\pi/\gamma\sqrt{e})k_{\rm B}T_{\rm c}^{(j)}$, leading to a gap maximum to $T_{\rm c}$ ratio of 4.28, instead of the ratio 3.52 in the conventional case. For $T \ll T_{\rm c}$ the unconventional gap decreases from its $T = 0$ value as $|\Delta_j(T)/\Delta_j(0)| = 1 - 3\zeta(3)[k_{\rm B}T/|\Delta_j(0)|]^3$, which is to be contrasted with the exponential correction for a constant gap. Similar power law behavior is found for other quantities as well, due to the line nodes in the excitation spectrum. For example the specific heat vanishes like T^2 at low temperatures, and normalized

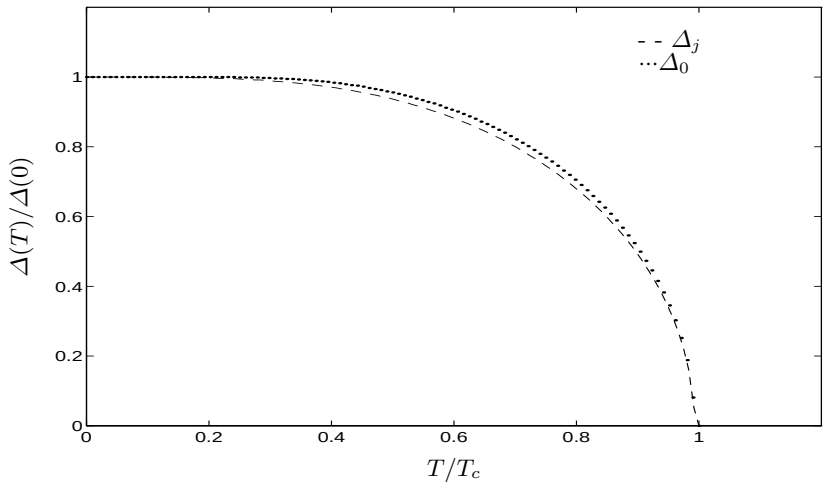

Fig. 3. The temperature dependence of the gap amplitude for conventional (dotted line) and unconventional (dashed line) density wave.

to the normal state value we obtain $C_v^{(j)}(T)/C_v^{(n)}(T) = [27\zeta(3)/\pi^2][k_{\rm B}T/|\Delta_j(0)|]$, as opposed to the exponential freezing out for a conventional gap. Close to the transition temperature the unconventional gap vanishes like $[|\Delta_j(T)|/k_{\rm B}T_{\rm c}^{(j)}]^2 = [32\pi^2/21\zeta(3)][1 - T/T_{\rm c}^{(j)}]$, *i.e.* in a square root manner with somewhat different prefactor compared to the conventional case ($8\pi^2/7\zeta(3)$). The mean field transition leads to a specific heat jump at $T_{\rm c}$ with the relative value of $\Delta C_v^{(j)}/C_v^{(n)} = 8/7\zeta(3) = 0.95$, exactly two third of the conventional value. Due to the presence of line nodes in the gap function the above thermodynamic properties are identical to those of a $d_{x^2-y^2}$ superconductor [3] in spite of the different topology of their Fermi surfaces.

3 Correlation functions and the nature of the order parameter

At this point it is important to call the attention to the fact that while in a conventional SDW the order parameter is proportional to the Fourier component of the magnetization density at the nesting vector $\mathbf{Q}$, an unconventional order parameter has nothing to do with the magnetization. In order to see this we evaluate the magnetization using the transformation in equation (8):

$$\langle m(\mathbf{Q})\rangle = -\mu_{\rm B}\sum_{\mathbf{k},\sigma}{}' \sigma\langle a^+_{\mathbf{k}-\mathbf{Q},\sigma}a_{\mathbf{k},\sigma}\rangle = \mu_{\rm B}\sum_{\mathbf{k}}{}' \frac{\Delta(\mathbf{k})\tanh\left\{\frac{\beta}{2}E(\mathbf{k})\right\}}{E(\mathbf{k})}\,. \qquad (18)$$

It is easily seen that equation (18) yields zero magnetization for any of the four unconventional gap functions, as opposed to the conventional situation leading to $\langle m(\mathbf{Q})\rangle = 2N\mu_{\rm B}\Delta_0/P_0$. This means that an USDW is *not* accompanied by a spatially periodic modulation of the spin density, although the expectation value $\langle a^+_{\mathbf{k}-\mathbf{Q},\sigma}a_{\mathbf{k},\sigma}\rangle$ becomes finite and the existence of a robust thermodynamic phase transition is unquestionable. This feature of the unconventional density waves makes them suitable candidates for explaining low temperature phase transitions, where conventional order parameters such as charge-, or spin-density modulation are not observable, like in α-(BEDT-TTF)$_2$KHg(SCN)$_4$ [14], or in URu$_2$Si$_2$ [5] respectively.

What kind of physical quantity does then an unconventional gap correspond to? Again utilizing the gap equation (11), we can convince ourselves that if for example an unconventional gap $\Delta_1\cos(k_y b)$ develops at low temperature, then the quantity

$$\tilde{S}_z(\mathbf{q}) = \frac{1}{2}\sum_{\mathbf{k},\sigma}\sigma\sin[b(k_y + q_y/2)]a^+_{\mathbf{k},\sigma}a_{\mathbf{k}+\mathbf{q},\sigma} \qquad (19)$$

assumes a finite expectation value $\langle\tilde{S}_z(\mathbf{Q})\rangle = N\Delta_1/P_1$. Therefore the Fourier component with wavenumber $\mathbf{Q}$ of the "effective" spin density $\tilde{S}_z(\mathbf{r})$ plays the role of the order parameter in this unconventional case. Clearly, experimental observation of this order parameter is possible only in probes coupling directly to this physical quantity. The situation is rather similar to electronic Raman scattering, where the photon-electron vertex carries momentum dependence, and measures the effective density correlation function [9,10], instead of scattering on just density fluctuations. Equation (19), and its real space version suggests that $\tilde{S}_z$ is in fact the spin current density, and the low temperature phase is related to the so called spin nematic phase [28].

The rest of this chapter will be devoted to the evaluation of certain correlation functions which are of particular interest. We begin with the charge susceptibility $\chi_{nn}(\mathbf{q},t) = {\rm i}\langle[n(\mathbf{q},t), n(-\mathbf{q},0)]\rangle$, the autocorrelation function of the density operator $n(\mathbf{q}) = \sum_{\mathbf{k},\sigma}a^+_{\mathbf{k},\sigma}a_{\mathbf{k}+\mathbf{q},\sigma}$. The quasiparticle contribution to the frequency dependent

charge susceptibility in the long wavelength limit reads as

$$\chi_{nn}(\mathbf{q},\omega) = \frac{1}{V}\sum_{\mathbf{k},\sigma}{}' \left[\frac{1}{2}\left(1+\frac{\xi(\mathbf{k})\xi(\mathbf{k}+\mathbf{q})+\mathrm{Re}(\overline{\Delta(\mathbf{k})}\Delta(\mathbf{k}+\mathbf{q}))}{E(\mathbf{k})E(\mathbf{k}+\mathbf{q})}\right) \times\{f[E(\mathbf{k}+\mathbf{q})]-f[E(\mathbf{k})]\} \times\left(\frac{1}{\omega+E(\mathbf{k})-E(\mathbf{k}+\mathbf{q})}-\frac{1}{\omega-E(\mathbf{k})+E(\mathbf{k}+\mathbf{q})}\right) + \frac{1}{2}\left(1-\frac{\xi(\mathbf{k})\xi(\mathbf{k}+\mathbf{q})+\mathrm{Re}(\overline{\Delta(\mathbf{k})}\Delta(\mathbf{k}+\mathbf{q}))}{E(\mathbf{k})E(\mathbf{k}+\mathbf{q})}\right) \times\{1-f[E(\mathbf{k}+\mathbf{q})]-f[E(\mathbf{k})]\} \times\left(\frac{1}{\omega+E(\mathbf{k})+E(\mathbf{k}+\mathbf{q})}-\frac{1}{\omega-E(\mathbf{k})-E(\mathbf{k}+\mathbf{q})}\right)\right], \tag{20}$$

while for wavenumbers around the nesting vector we obtain

$$\begin{aligned}\chi_{nn}(\mathbf{Q}+\mathbf{q},\omega) = \frac{1}{4V}\sum_{\mathbf{k},\sigma}{}' \Bigg[& \frac{f[E(\mathbf{k}+\mathbf{q})]-f[E(\mathbf{k})]}{\omega+E(\mathbf{k})-E(\mathbf{k}+\mathbf{q})} \times\left(1-\frac{\xi(\mathbf{k})}{E(\mathbf{k})}\right)\left(1+\frac{\xi(\mathbf{k}+\mathbf{q})}{E(\mathbf{k}+\mathbf{q})}\right) \\ & + \frac{f[E(\mathbf{k})]-f[E(\mathbf{k}+\mathbf{q})]}{\omega-E(\mathbf{k})+E(\mathbf{k}+\mathbf{q})} \times\left(1+\frac{\xi(\mathbf{k})}{E(\mathbf{k})}\right)\left(1-\frac{\xi(\mathbf{k}+\mathbf{q})}{E(\mathbf{k}+\mathbf{q})}\right) \\ & + \frac{1-f[E(\mathbf{k})]-f[E(\mathbf{k}+\mathbf{q})]}{\omega+E(\mathbf{k})+E(\mathbf{k}+\mathbf{q})} \times\left(1-\frac{\xi(\mathbf{k})}{E(\mathbf{k})}\right)\left(1-\frac{\xi(\mathbf{k}+\mathbf{q})}{E(\mathbf{k}+\mathbf{q})}\right) \\ & + \frac{f[E(\mathbf{k})]+f[E(\mathbf{k}+\mathbf{q})]-1}{\omega-E(\mathbf{k})-E(\mathbf{k}+\mathbf{q})} \times\left(1+\frac{\xi(\mathbf{k})}{E(\mathbf{k})}\right)\left(1+\frac{\xi(\mathbf{k}+\mathbf{q})}{E(\mathbf{k}+\mathbf{q})}\right)\Bigg]. \end{aligned} \tag{21}$$

Since the above two equations correspond to bubble diagrams, the analytic structure of the spin susceptibilities are very similar to equations (20) and (21). For example the longitudinal spin susceptibility $\chi_{S_zS_z} = \chi_{nn}/4$ for all wavelengths, and the transverse spin susceptibility $\chi_{S^+S^-} = \chi_{nn}/2$ for short wavelengths. For long wavelengths however, we encounter coherence factors different from those in equation (20), namely the sign of the two $\mathrm{Re}(\overline{\Delta(\mathbf{k})}\Delta(\mathbf{k}+\mathbf{q}))$ terms becomes negative.

In the followings we evaluate the above mentioned correlation functions in both the static (first $\omega \to 0$, then $\mathbf{q} \to 0$), and the dynamic (first $\mathbf{q} \to 0$, then $\omega \to 0$) limit.

3.1 Susceptibilities in the long wavelength limit

The dynamic limit of the long wavelength charge susceptibility is trivially zero, therefore we begin with the static limit of equation (20):

$$\begin{aligned}\chi_{nn}^{0S} &= \frac{2}{V}\sum_{\mathbf{k},\sigma}{}'\{-f'[E(\mathbf{k})]\} \\ &= g_0(0)\int_{-\infty}^{\infty}\mathrm{d}E[-f'(E)]\rho(E)/\rho_0(0),\end{aligned} \tag{22}$$

where $f'(E)$ is the derivative of the Fermi function, and $g_0(0) = 2N\rho_0(0)/V$ is the normal state DOS (per unit volume) at the Fermi energy including spin degeneracy. The above susceptibility takes this value for $T > T_\mathrm{c}$, and its temperature dependence is shown in Figure 4 for both the conventional and the unconventional cases. We note here, that following superconductivity terminology, equation (22) is often expressed as $\chi_{nn}^{0S} = g_0(0)(1-f_s)$, where f_s is the superfluid fraction. In our case of course, condensate fraction is more appropriate. Due to the above mentioned relations between correlation functions, Figure 4 represents also the longitudinal spin susceptibility, experimentally accessible through Knight-shift measurement, vanishing at low temperatures. This is in contrast to the static homogeneous transverse spin susceptibility $\chi_{S^+S^-}^{0S} = V^{-1}\sum_{\mathbf{k}}'|\Delta(\mathbf{k})|^2/[E(\mathbf{k})]^3 = g_0(0)/2$, which turns out to be independent of the gap, and consequently of the temperature. Returning to the charge (or longitudinal spin) susceptibility, equation (22) is evaluated at low temperatures yielding exponential freezeout for conventional SDW, and $\chi_{nn}^{0S}/g_0(0) = 2\ln(2)k_\mathrm{B}T/|\Delta_j(0)|$ for the USDW. Close to T_c on the other hand $\chi_{nn}^{0S}/g_0(0) = (4T/T_\mathrm{c}^{(j)}-1)/3$ for USDW (instead of the conventional value $2T/T_\mathrm{c}^{(0)}-1$).

Wrapping up our discussion of the long wavelength correlation functions, we consider the dynamic limit of the transverse spin susceptibility

$$\begin{aligned}\chi_{S^+S^-}^{0D} &= \frac{1}{V}\sum_{\mathbf{k}}{}'\frac{|\Delta(\mathbf{k})|^2}{[E(\mathbf{k})]^3}\{1-2f[E(\mathbf{k})]\} \\ &= \frac{g_0(0)}{2}\int_0^\infty \mathrm{d}E\frac{1-2f(E)}{E^2} \\ &\quad\times\int_{-\pi}^{\pi}\frac{\mathrm{d}(bk_y)}{2\pi}\int_{-\pi}^{\pi}\frac{\mathrm{d}(ck_z)}{2\pi}\mathrm{Re}\frac{|\Delta(\mathbf{k})|^2}{\sqrt{E^2-|\Delta(\mathbf{k})|^2}},\end{aligned} \tag{23}$$

which is nonzero in the DW state, as shown in Figure 5 for both conventional and unconventional situations. The susceptibility normalized to its zero temperature value $\chi_{S^+S^-}^{0D}(T)/[g_0(0)/2] = f_d$ is again the condensate fraction, but now in the dynamic limit. In order to see the difference compared to the static condensate fraction, we first realize that $[g_0(0)/4](f_d-f_s) = V^{-1}\sum_{\mathbf{k}}'\{-f'[E(\mathbf{k})]\}|\Delta(\mathbf{k})|^2/[E(\mathbf{k})]^2$, then consider the limiting values for low and high temperatures. For $T \to 0$ the dynamic

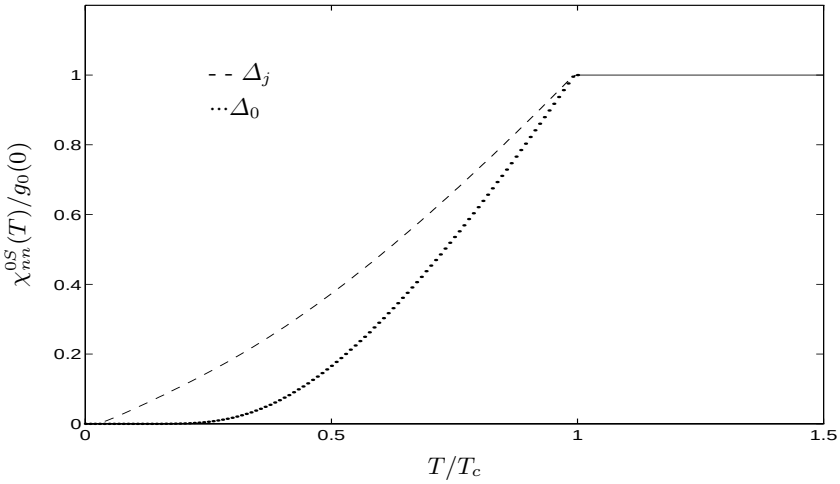

Fig. 4. The temperature dependence of the long wavelength static charge susceptibility χ^{0S}_{nn} for conventional (dotted line) and for unconventional (dashed line) density waves.

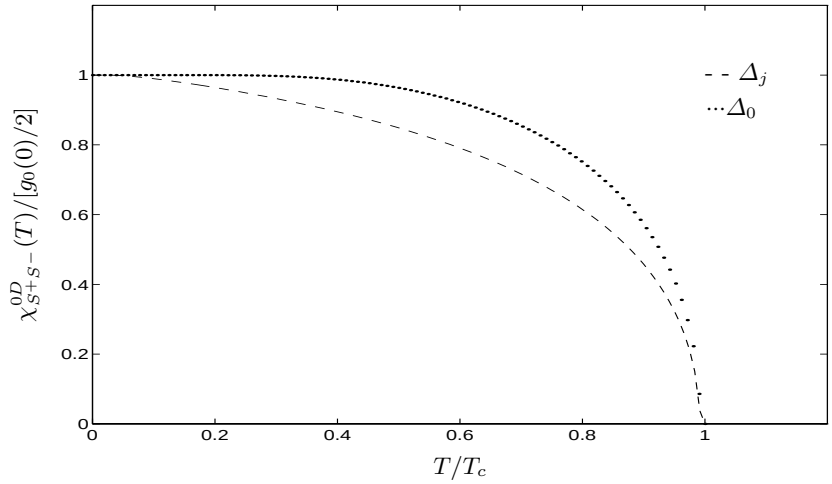

Fig. 5. The temperature dependence of the long wavelength dynamic transverse spin susceptibility $\chi^{0D}_{S^+S^-}$ for conventional (dotted line) and for unconventional (dashed line) density waves.

condensate fraction $f_d = 1 - \ln(2)k_{\rm B}T/|\Delta_j(0)|$ in USDW (the finite temperature correction is exponentially small for the conventional case). Close to $T_{\rm c}$ the dynamic condensate fraction vanishes like $\pi|\Delta_0|/4k_{\rm B}T$ for constant gap, and like $|\Delta_j|/2k_{\rm B}T$ for momentum dependent gap.

3.2 Susceptibilities around the nesting vector

We turn our attention now to the behavior of the short wavelength correlation functions based on equation (21). These are of particular interest in describing phenomena related to the phase transition involving the nesting vector $\mathbf{Q}$. It is easily seen, that in the normal state ($T > T_{\rm c}$) the charge susceptibility at the nesting vector follows a logarithmic temperature dependence

$$\chi^{Q}_{nn} = \frac{1}{V}\sum_{\mathbf{k},\sigma}{}' \frac{1-2f[\xi(\mathbf{k})]}{2\xi(\mathbf{k})} = \frac{g_0(0)}{2}\ln\frac{2\gamma v_{\rm F}k_{\rm F}}{\pi k_{\rm B}T} \qquad (24)$$

for both conventional and unconventional cases independent of the limiting procedure (static or dynamic).

Below the transition temperature we obtain a still rather simple formula

$$\chi^{Q}_{nn} = \frac{1}{V}\sum_{\mathbf{k},\sigma}{}' \frac{1-2f[E(\mathbf{k})]}{2E(\mathbf{k})} - \frac{g_0(0)}{4}f, \qquad (25)$$

incorporating all the variations in the condensate fraction f, discussed extensively in the previous subsection in all limits and cases. It is easy to deal with the first term in equation (25) for a constant gap, since the gap equation (11) relates just such an expression with the inverse of the coupling constant. Therefore in the conventional case $\chi^{Q}_{nn} = 2N/VP_0 - [g_0(0)/4]f$, leading to a monotonically decreasing susceptibility in both the static and dynamic limit as the temperature is lowered (see Figs. 6 and 7).

In case of a momentum dependent gap, the first term in equation (25) is not exactly what appears in the gap equation (11), but at the expense of a correction factor

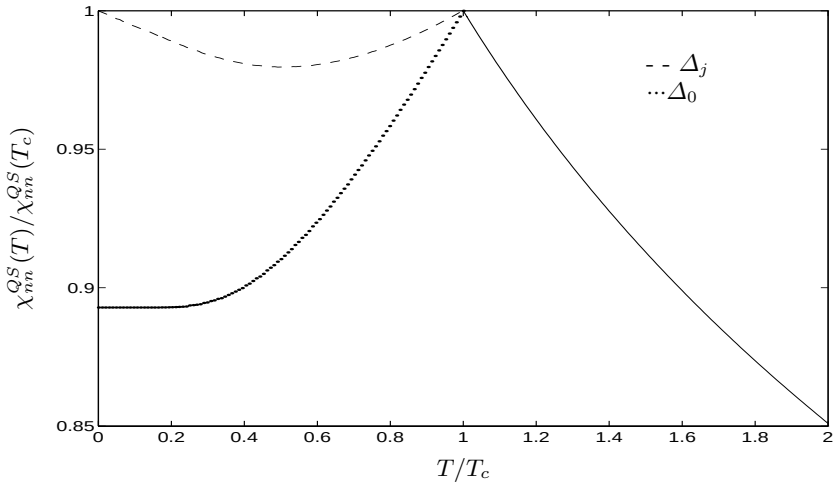

Fig. 6. The temperature dependence of the short wavelength charge susceptibility χ^Q_{nn} in the static limit for conventional (dotted line) and for unconventional (dashed line) density waves. We have chosen $P_0\rho_0(0) = P_j\rho_0(0)/2 \approx 0.43$.

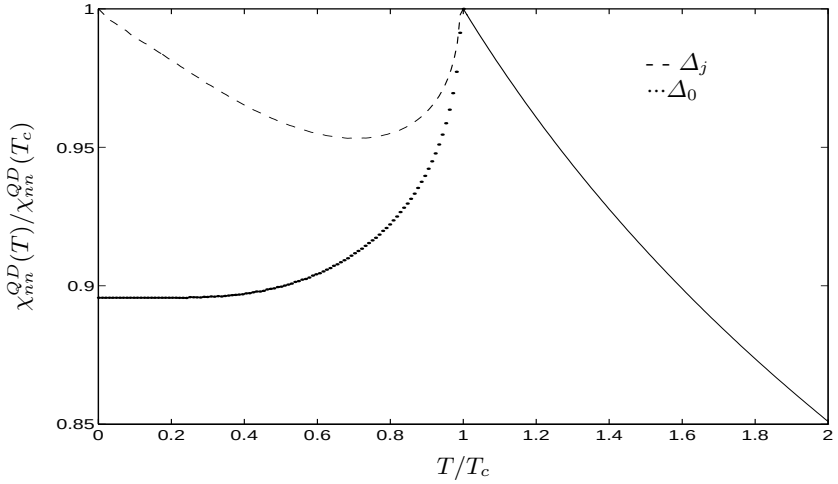

Fig. 7. The temperature dependence of the short wavelength charge susceptibility χ^Q_{nn} in the dynamic limit for conventional (dotted line) and for unconventional (dashed line) density waves. Coupling constants are chosen as in Figure 6.

we can bring in the inverse coupling constant as in the conventional case: $\chi^Q_{nn} = 4N/VP_j - [g_0(0)/4](f - \delta f)$, where

$$\delta f = 4\int_{-\pi}^{\pi}\frac{\mathrm{d}(bk_y)}{2\pi}\int_{-\pi}^{\pi}\frac{\mathrm{d}(ck_z)}{2\pi} \times \int_0^{v_\mathrm{F}k_\mathrm{F}}\mathrm{d}E\mathrm{Re}\frac{1-2f(E)}{\sqrt{E^2-|\Delta(\mathbf{k})|^2}}\left[\frac{1}{2}-\left|\frac{\Delta(\mathbf{k})}{\Delta_j}\right|^2\right]. \quad (26)$$

This correction factor is evaluated as $\delta f = 1 - 4\ln(2)k_\mathrm{B}T/|\Delta_j(0)|$ for low temperatures, and as $\delta f = (2/3)(1 - T/T_\mathrm{c}^{(j)})$ close to the critical temperature.

Our results concerning the susceptibility at the nesting vector are summarized in Figures 6 and 7 for the static and dynamic limits respectively. In the conventional situation $\chi^Q_{nn} \propto \chi^Q_{S_zS_z}$ is peaked at the critical temperature signaling the phase transition. Indeed, if we consider the full spin susceptibility in random phase approximation (RPA), the Stoner denominator vanishes exactly if we approach $T_\mathrm{c}^{(0)}$ from above, leading to divergent response. The other (unconventional) coupling channels do not contribute to the charge (spin) response due to their momentum dependence. In the unconventional case however, RPA corrections will not lead to divergence, since the dominant unconventional channel does not couple to charge or spin density, while the conventional coupling constant is not strong enough to make the Stoner denominator vanish. Instead, the autocorrelation function of the effective spin density $\tilde{S}_z$ (see *e.g.* Eq. (19)) will be divergent at $T_\mathrm{c}^{(j)}$ in RPA, as it should if we are to have an unconventional phase transition.

4 Optical conductivity

The frequency dependent conductivity provides a wealth of information about both the quasiparticle and the collective excitation spectrum of density wave materials [1]. Therefore in this section we investigate the properties of

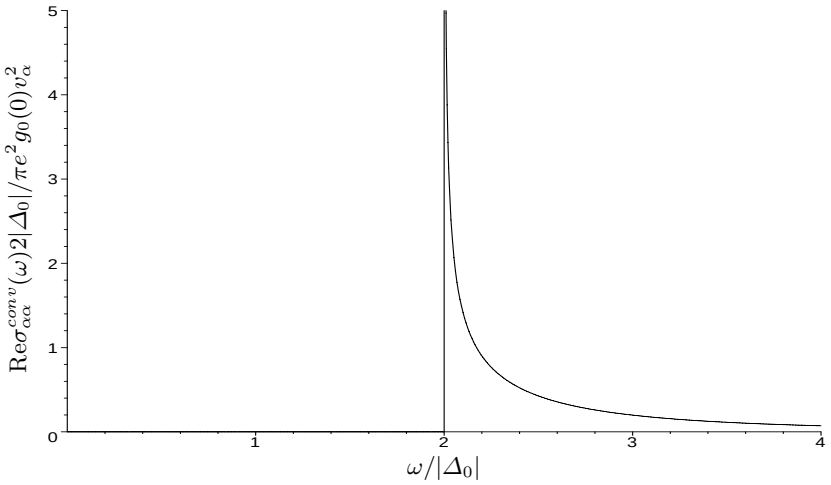

Fig. 8. The real part of the complex conductivity of a conventional SDW at $T = 0$.

the conductivity tensor $\sigma_{\alpha\beta}(\omega) = K_{\alpha\beta}(\mathbf{q} = 0, \omega)/\mathrm{i}\omega$ in our model of USDW. The electromagnetic kernel consists of so called paramagnetic and diamagnetic parts: $K_{\alpha\beta} = K^P_{\alpha\beta} + K^D_{\alpha\beta}$. The diamagnetic term $K^D_{\alpha\beta} = -e^2 V^{-1} \sum'_{\mathbf{k},\sigma} m^{-1}_{\alpha\beta}(\mathbf{k})$ involves the effective mass tensor derived from the electronic spectrum (2). The paramagnetic part $K^P_{\alpha\beta} = \chi_{j_\alpha j_\beta}$ is the correlation function of the corresponding components of the current operator given by $\mathbf{j}(\mathbf{q}) = -e \sum_{\mathbf{k},\sigma} \mathbf{v}(\mathbf{k}) a^+_{\mathbf{k},\sigma} a_{\mathbf{k}+\mathbf{q},\sigma}$ in the $\mathbf{q} \to 0$ limit, where the electron velocity is again obtained from equation (2). The current correlation function turns out to be given by the same formula as in equation (20), except for the different coherence factors and the multiplicative term $e^2 v_\alpha(\mathbf{k}) v_\beta(\mathbf{k})$ under the summation. Since our system is ideal in a sense that it does not include any source of damping for electrons (for example impurity scattering), the real part of the conductivity consists of a sharp Drude peak and a regular contribution: $\mathrm{Re}\sigma_{\alpha\beta}(\omega) = \pi D_{\alpha\beta}\delta(\omega) + \mathrm{Re}\sigma^{\mathrm{reg}}_{\alpha\beta}(\omega)$, where the Drude weight is given by

$$D_{\alpha\beta} = \frac{e^2}{V} \sum_{\mathbf{k},\sigma}{}' \left\{ m^{-1}_{\alpha\beta}(\mathbf{k}) - v_\alpha(\mathbf{k}) v_\beta(\mathbf{k}) \frac{|\Delta(\mathbf{k})|^2}{[E(\mathbf{k})]^3} \{1 - 2f[E(\mathbf{k})]\} \right\}. \quad (27)$$

The Drude peak is the only component in the normal state, but its weight decreases below T_c and vanishes completely at zero temperature. For example in the chain direction the Drude wight is related to the dynamic condensate fraction by $D_{xx} = e^2 g_0(0) v_\mathrm{F}^2 (1 - f_d)$. The missing oscillator strength is taken over by the regular component at finite frequencies:

$$\mathrm{Re}\sigma^{\mathrm{reg}}_{\alpha\beta}(\omega) = g_0(0) \frac{\pi e^2}{\omega^2} \tanh\left(\frac{|\omega|}{4k_\mathrm{B}T}\right) \times \int_{-\pi}^{\pi} \frac{\mathrm{d}(bk_y)}{2\pi} \int_{-\pi}^{\pi} \frac{\mathrm{d}(ck_z)}{2\pi} \mathrm{Re} \frac{v_\alpha(\mathbf{k}) v_\beta(\mathbf{k}) |\Delta(\mathbf{k})|^2}{\sqrt{(\omega/2)^2 - |\Delta(\mathbf{k})|^2}}. \quad (28)$$

In order to obtain characteristic lineshapes for the optical conductivity tensor, we first realize that it is diagonal, then consider various gap functions and electric field directions. In case of a conventional SDW the conductivity is given by

$$\mathrm{Re}\sigma^{\mathrm{conv}}_{\alpha\alpha}(\omega > 0) = e^2 g_0(0) v_\alpha^2 \tanh\left(\frac{\omega}{4k_\mathrm{B}T}\right) \times \frac{\pi |\Delta_0|^2}{\omega^2} \mathrm{Re} \frac{1}{\sqrt{(\omega/2)^2 - |\Delta_0|^2}}, \quad (29)$$

where $v_x = v_\mathrm{F}$, $v_y = \sqrt{2} b t_b$ and $v_z = \sqrt{2} c t_c$. The frequency dependence of the conductivity is the same for all three directions of the electric field, and is shown in Figure 8 at zero temperature. We recognize the sharp onset of absorption at $\omega = 2|\Delta_0|$ due to the constant gap.

In the unconventional situations we expect finite absorption below the maximum gap, since we have low energy optical excitations around the nodes of the order parameter. Consider first the conductivity in the chain direction

$$\mathrm{Re}\sigma^{\mathrm{unc}}_{xx}(\omega > 0) = e^2 g_0(0) v_\mathrm{F}^2 \tanh\left(\frac{\omega}{4k_\mathrm{B}T}\right) \frac{4|\Delta_j|^2}{\omega^3} I\left(\frac{2|\Delta_j|}{\omega}\right), \quad (30)$$

where $I(k) = \int_0^{\pi/2} \mathrm{d}\varphi \sin^2\varphi \mathrm{Re}(1 - k^2 \sin^2\varphi)^{-1/2}$, evaluated as $I(k < 1) = [K(k) - E(k)]/k^2$, and $I(k > 1) = [K(1/k) - E(1/k)]/k$. This function is plotted in Figure 9 at zero temperature. We see a logarithmic divergence at the maximum optical gap, and a substantial absorption below that gap as expected. We note here, that if we consider the conductivity in one of the directions perpendicular to the chain, we obtain the same lineshape if the unconventional gap varies in the other perpendicular direction. Of course we need to replace v_F in equation (30) by the proper perpendicular velocity. At this point it is appropriate to remark that we are calculating only quasiparticle contributions to the conductivity, although it is

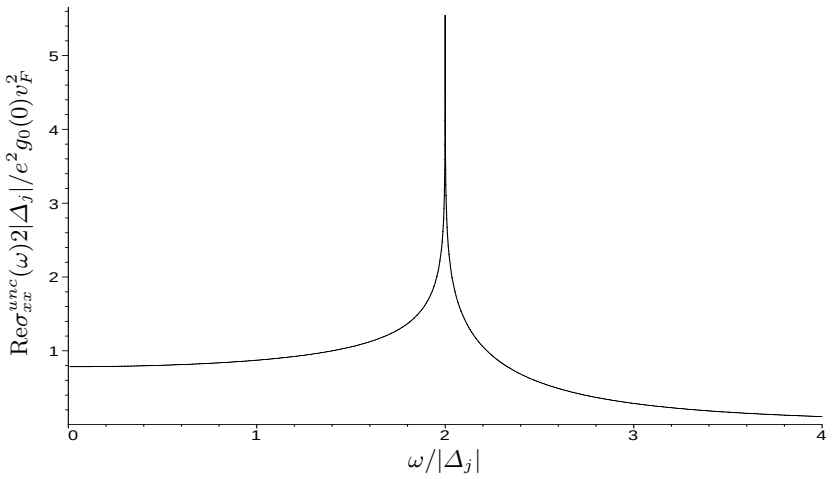

Fig. 9. The real part of the complex conductivity of an USDW in the chain direction at $T = 0$.

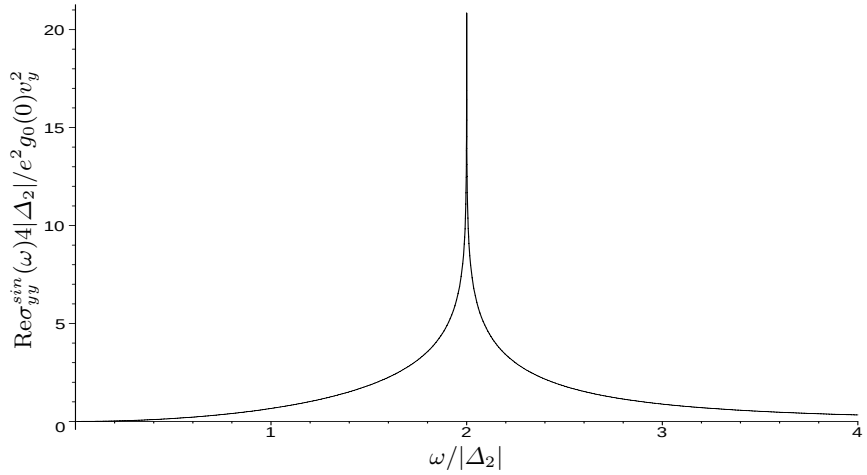

Fig. 10. The real part of the complex conductivity of an USDW in the y-direction at $T = 0$, $\Delta(\mathbf{k}) = \Delta_2 \sin(k_y b)$.

known that due to the sliding motion of the condensate a collective contribution will also be observed in the chain direction [32]. For example the quasiparticle peak on Figure 8 will be absorbed by the phason at much lower frequencies. However, if the electric field is perpendicular to the chains, no such contribution is expected, therefore our results are directly applicable to the experimental situation.

Finally, we consider the situation when the electric field is aligned in that perpendicular direction in which the order parameter varies. Without loss of generality we can take this to be the y-direction. There are two possibilities corresponding to the gap function $\Delta(\mathbf{k}) = \Delta_1 \cos(k_y b)$, and $\Delta(\mathbf{k}) = \Delta_2 \sin(k_y b)$. Equation (28) leads to the following expressions for the conductivities:

$$\mathrm{Re}\sigma_{yy}^{\cos}(\omega > 0) = e^2 g_0(0) v_y^2 \tanh\left(\frac{\omega}{4k_{\mathrm{B}}T}\right) \frac{8|\Delta_1|^2}{\omega^3} I_{\cos}\left(\frac{2|\Delta_1|}{\omega}\right), \quad (31)$$

and

$$\mathrm{Re}\sigma_{yy}^{\sin}(\omega > 0) = e^2 g_0(0) v_y^2 \tanh\left(\frac{\omega}{4k_{\mathrm{B}}T}\right) \frac{8|\Delta_2|^2}{\omega^3} I_{\sin}\left(\frac{2|\Delta_2|}{\omega}\right), \quad (32)$$

where $I_{\sin}(k) = \int_0^{\pi/2} \mathrm{d}\varphi \sin^4\varphi \mathrm{Re}(1 - k^2\sin^2\varphi)^{-1/2}$, and $I_{\cos}(k) = I(k) - I_{\sin}(k)$. The former function is evaluated as $I_{\sin}(k < 1) = [(2 + k^2)K(k) - 2(1 + k^2)E(k)]/3k^4$, and $I_{\sin}(k > 1) = [(1 + 2k^2)K(1/k) - 2(1 + k^2)E(1/k)]/3k^3$. We plot these results in Figure 10 and in Figure 11 for the sine and cosine dependence of the order parameter respectively. As seen on Figure 10, due to the matching of the $\mathbf{k}$ dependences of the gap and the velocity $v_y(\mathbf{k}) = 2bt_b \sin(k_y b)$ the low frequency conductivity is suppressed and proportional to ω^2, while the logarithmic divergence is still there at $\omega = 2|\Delta_2|$, as for the chain direction conductivity (see Fig. 9). This reasoning is quite similar to the one used in explaining the lineshape of the B_{1g} Raman response in $d_{x^2-y^2}$ superconductors [33].

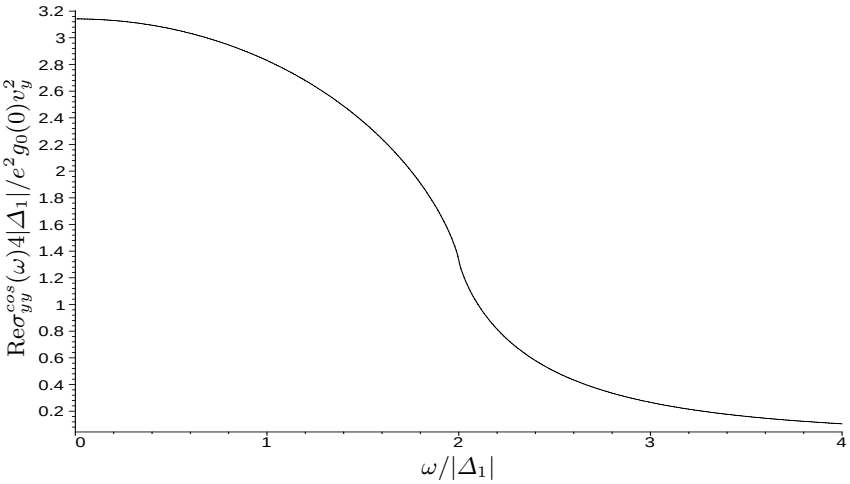

Fig. 11. The real part of the complex conductivity of an USDW in the y-direction at $T = 0$, $\Delta(\mathbf{k}) = \Delta_1 \cos(k_y b)$.

In case of a cosine gap on the other hand, the velocity is zero at the gap maximum, therefore the logarithmic divergence is cut off at $\omega = 2|\Delta_1|$, and we have a monotonically decreasing conductivity as shown in Figure 11.

5 Conclusions

In this paper we have developed the mean field theory of unconventional density waves in quasi-one-dimensional interacting electron systems. Although our calculations refer explicitly to unconventional spin density waves (USDW), most of the results apply to unconventional charge density waves as well. We have found that the excitation spectrum and thermodynamics of our model are identical to those of a d-wave superconductor, due to the presence of line nodes in the gap function $\Delta(k_y, k_z)$. Formation of an USDW is facilitated by a combination of interchain Coulomb and exchange integrals overwhelming the on site repulsion.

It is important to realize that an USDW is not accompanied by a spatially periodic modulation of the spin density. Instead, an effective spin density plays the role of the order parameter, which is observable only in probes coupling to this quantity through form factors significantly dependent on wavenumber. This feature of the unconventional density waves makes them suitable candidates for explaining low temperature phase transitions, where conventional order parameters such as charge-, or spin-density modulation are not observable. This state of affairs is sometimes referred to as "hidden order" in the context of for example URu_2Si_2 [7], and may be responsible for the mysterious low temperature phase in α-$(ET)_2$ salts [14], where neither (conventional) charge, nor spin order has been established firmly by either X-ray or NMR probes in spite of the presence of a quasi-one-dimensional part of their Fermi surface. The above conclusion is also corroborated by our investigation of charge and spin correlation functions at the nesting vector, which do not diverge at the critical temperature in random phase approximation, unlike the effective spin density correlator, which does. The homogeneous static spin susceptibility shows qualitatively the same anisotropic behavior below the transition temperature as in the conventional case.

Finally, we have calculated the quasiparticle contribution to the frequency dependent conductivity for an USDW system without quasiparticle damping (collisionless limit). The lineshape always exhibits absorption for frequencies below the maximum optical gap in the quasiparticle spectrum, but varies significantly depending on the direction of the electric field and on the functional form of the gap function. These differences can be exploited in determining the nature of the condensate by optical spectroscopic tools.

This work was supported by the Hungarian National Research Fund under grant numbers OTKA T032162 and T029877, and by the Ministry of Education under grant number FKFP 0029/1999.

References

1. G. Grüner, *Density waves in solids* (Addison-Wesley, Reading, 1994).
2. P.W. Anderson, P. Morel, Phys. Rev. **123**, 1911 (1961).
3. K. Maki, in *Lectures in the Physics of Highly Correlated Electron Systems*, edited by F. Mancini, *AIP Conference Proceedings 438*, *Woodbury*, *1998*, p. 83.
4. Z. Gulácsi, M. Gulácsi, Phys. Rev. B **36**, 699 (1987).
5. E.D. Isaacs, D.B. McWhan, R.N. Kleiman, D.J. Bishop, G.E. Ice, P. Zschack, B.D. Gaulin, T.E. Mason, J.D. Garrett, W.J.L. Buyers, Phys. Rev. Lett. **65**, 3185 (1990).
6. V. Barzykin, L.P. Gor'kov, Phys. Rev. Lett. **70**, 2479 (1993).
7. N. Shah, P. Chandra, P. Coleman, J.A. Mydosh, Phys. Rev. B **61**, 564 (2000).
8. H. Ikeda, Y. Ohasi, Phys. Rev. Lett. **81**, 3723 (1998).
9. A.A. Abrikosov, V.M. Genkin, Sov. Phys. JETP **38**, 417 (1974).

10. T.P. Devereaux, A. Virosztek, A. Zawadowski, Phys. Rev. B **54**, 12523 (1996).
11. L. Degiorgi, S. Thieme, H.R. Ott, M. Dressel, G. Grüner, Y. Dalichaouch, M.B. Maple, Z. Fisk, C. Geibel, F. Steglich, Z. Phys. B **102**, 367 (1997).
12. H. Guyot, E.A. Khoury, J. Marcus, C. Schlenker, M. Banville, S. Jandl, Sol. State Commun. **79**, 307 (1991).
13. A.W. McConnell, B.P. Clayman, C.C. Homes, M. Inoue, H. Negishi, Phys. Rev. B **58**, 13565 (1998).
14. P. Christ, W. Biberacher, M.V. Kartsovnik, E. Steep, E. Balthes, H. Weiss, H. Müller, JETP Lett. **71**, 303 (2000).
15. C. Proust, A. Audouard, A. Kovalev, D. Vignolles, M. Kartsovnik, L. Brossard, N. Kushch, Phys. Rev. B **62**, 2388 (2000).
16. M.V. Kartsovnik, D. Andres, W. Biberacher, P. Christ, E. Steep, E. Balthes, H. Weiss, H. Müller, N.D. Kushch, Synth. Metals **120**, 687 (2001).
17. R. Liu, C.G. Olson, W.C. Tonjes, R.F. Frindt, Phys. Rev. Lett. **80**, 5762 (1998).
18. D.C. Johnston, M. Maki, G. Grüner, Sol. State Commun. **53**, 1 (1985).
19. L. Németh, P. Matus, G. Kriza, B. Alavi, Synth. Metals **120**, 1007 (2001).
20. S. Chakravarty, R.B. Laughlin, D.K. Morr, C. Nayak, Phys. Rev. B **63**, 094503 (2001), `cond-mat/0005443`.
21. F. Bouis, M.N. Kiselev, F. Onufrieva, P. Pfeuty, Physica B **284-288**, 677 (2000).
22. C. Nayak, Phys. Rev. B **62**, 4880 (2000).
23. B.I. Halperin, T.M. Rice, in *Solid State Physics*, edited by F. Seitz, D. Turnbull, H. Ehrenreich (Academic Press, New York, 1968), Vol. 21, p. 115.
24. I.E. Dzyaloshinskii, V.M. Yakovenko, Sov. Phys. JETP **67**, 844 (1988).
25. I.E. Dzyaloshinskii, V.M. Yakovenko, Int. J. Mod. Phys **2**, 667 (1988).
26. H.J. Schulz, Phys. Rev. B **39**, 2940 (1989).
27. A.A. Nersesyan, G.E. Vachnadze, J. Low T. Phys. **77**, 293 (1989).
28. A.A. Nersesyan, G.I. Japaridze, I.G. Kimeridze, J. Phys. Cond. Matt. **3**, 3353 (1991).
29. A.A. Nersesyan, Phys. Lett. A **153**, 49 (1991).
30. B. Dóra, A. Virosztek, J. Phys. IV France **9**, Pr10-239 (1999).
31. M. Ozaki, Int. J. Quantum Chem. **42**, 55 (1992).
32. A. Virosztek, K. Maki, Phys. Rev. B **37**, 2028 (1988).
33. T.P. Devereaux, D. Einzel, B. Stadlober, R. Hackl, D.H. Leach, J.J. Neumeier, Phys. Rev. Lett. **72**, 396 (1994).